

Dalton Transactions

Accepted Manuscript



This is an *Accepted Manuscript*, which has been through the Royal Society of Chemistry peer review process and has been accepted for publication.

Accepted Manuscripts are published online shortly after acceptance, before technical editing, formatting and proof reading. Using this free service, authors can make their results available to the community, in citable form, before we publish the edited article. We will replace this *Accepted Manuscript* with the edited and formatted *Advance Article* as soon as it is available.

You can find more information about *Accepted Manuscripts* in the [Information for Authors](#).

Please note that technical editing may introduce minor changes to the text and/or graphics, which may alter content. The journal's standard [Terms & Conditions](#) and the [Ethical guidelines](#) still apply. In no event shall the Royal Society of Chemistry be held responsible for any errors or omissions in this *Accepted Manuscript* or any consequences arising from the use of any information it contains.

ARTICLE

Probing Ferroic Transitions in a Multiferroic Framework Family: A Neutron Diffraction Study of the Ammonium Transition Metal Formates

Cite this: DOI: 10.1039/x0xx00000x

James M. M. Lawler,^a Pascal Manuel,^b Amber L. Thompson^a and Paul. J. Saines*^aReceived 00th January 2012,
Accepted 00th January 2012

DOI: 10.1039/x0xx00000x

www.rsc.org/

This study probes the magnetic and ferroelectric ordering of the $\text{NH}_4\text{M}(\text{HCO}_2)_3$ ($\text{M} = \text{Mn}^{2+}$, Fe^{2+} , Co^{2+} and Ni^{2+}) frameworks using neutron diffraction, improving the understanding of the origins of the properties of these fascinating multiferroics. This rare study of the magnetic structure of a family of metal organic frameworks shows that all four compounds exhibit antiferromagnetic coupling between neighbouring cations bridged by formate ligands. The orientation of the spin, however, changes in a highly unusual way across the series with the spins aligned along the c -axis for the Fe^{2+} and Ni^{2+} frameworks but lying in the ab plane for the other members of the series. This work also sheds new light on the nature of the ferroelectric order-disorder transition in these materials; probing changes in the ammonium cation across the transition and also shows that the Ni^{2+} framework does not undergo a transition to the polar $P6_3$ phase due to the smaller size of the Ni^{2+} cation. Finally trends in their anisotropic negative thermal expansion, which potentially enhances their ferroic behaviour, are quantified.

Introduction

Functional magnets have tremendous potential to contribute to modern technologies in the form of multiferroic data storage,¹ magnetocaloric cooling^{2,3} and environmental sensors⁴. Such applications, however, require more complex and tuneable magnetic properties than can be provided by traditional magnetic compounds. This has recently led to significant interest in dense metal-organic frameworks (MOFs), whose magnetic properties have been shown to have great flexibility due to the wide range of unique architectures these materials can exhibit.^{3,5,6,7,8} The magnetic properties of such frameworks, however, depend on their precise magnetic interactions, which are poorly understood. It is crucial that this is rectified and the future development of magnetic MOFs be underpinned by a greater understanding of the origin of their properties.

Amongst MOFs the carboxylate frameworks, in particular those containing the formate ligand, have been shown to have significant potential as multiferroics,⁶ magnetocalorics^{3,9} and chemical sensors⁷. Of particular interest are the $\text{AB}(\text{HCO}_2)_3$ frameworks (where A is an large monovalent cations and B is a transition metal), which have been found to exhibit a unique mechanism for multiferrocity.^{6,10,11} Their ferroelectricity arises from ordering of the A-site cation due to hydrogen bond

interactions with the formate anions, which also bridge the magnetically ordered B-site cations. The structure adopted by the $\text{AB}(\text{HCO}_2)_3$ family changes significantly with increasing size of the A-site cation from a chiral hexagonal structure to a perovskite-like architecture to layered phases.^{6,10,11,12} The hexagonal phases adopted when the A-site cation is ammonium have $P6_322$ symmetry at ambient conditions but have previously all been reported to undergo a transition to a ferroelectric $P6_3$ phase at a relatively high temperature, amongst frameworks, near 200-250 K.^{11,13,14,15} Reported negative linear compressibility¹⁶ and anisotropic negative thermal expansion¹⁵ along the polar axis, in the Mg^{2+} and Zn^{2+} analogues, is indicative of behaviour that would reinforce the polarisation of the structure in the ferroelectric phase.

While the transition metal $\text{NH}_4\text{B}(\text{HCO}_2)_3$ compounds have been established by bulk measurements to be weak ferromagnets the magnetic interactions in the materials have not been examined in detail.^{11,13} Neutron diffraction has proved to be a powerful probe for examining such detailed magnetic interactions but its application to MOFs has been restricted to a handful of studies due to the low concentration of magnetic cations and the complex magnetic structures they often adopt.^{8,12,17} The greater sensitivity of neutron diffraction to hydrogen atoms also allows it to shed new light on the order-

disorder ferroelectric transition exhibited by this family. In this work we have used high quality neutron diffraction data to probe the magnetic structures across this series; a rare systematic study of the magnetic structures of a family of MOFs, which uncovers an unexpected alternation in their magnetic structures. We have also uncovered new details on the nature of the ferroelectric transition in this series and quantified the anisotropic negative thermal expansion of these compounds.

Experimental

Samples of $\text{NH}_4\text{B}(\text{HCO}_2)_3$ ($\text{B} = \text{Mn}^{2+}$, Co^{2+} , Fe^{2+} and Ni^{2+}) were made using an extensively modified version of the layered method utilised by Xu *et al.*,¹⁴ in which ammonium formate was used in place of aqueous ammonia (see ESI for further information). After the reaction conditions were optimised approximately 1 g samples of the Mn^{2+} , Co^{2+} and Ni^{2+} phases were made using perdeuterated reagents (all 98 % D) and used for neutron diffraction measurements; a deuterated sample of the Fe^{2+} analogue was not produced due to the significantly lower yields encountered during the synthesis. Phase purity of both the hydrogenated and deuterated products were determined using either a Philips PW 1729, equipped with a scintillator detector, or a PANalytical X'Pert Pro, equipped with an X'celerator linear detector; both instruments used $\text{Cu K}\alpha$ radiation. Single crystal diffraction measurements were performed using a Nonius KappaCCD diffractometer equipped with a liquid N_2 cryostream or I19 at the Diamond Light Source¹⁸ at 30 K, using an Oxford Cryosystems N-HeliX cryostream and a Rigaku Saturn 724+ CCD detector. The instruments used wavelengths of 0.7107 and 0.6889 Å, respectively, and samples were held on a MiTiGen perfluoropolyether microloop. Data collection strategies and processing for the Nonius diffractometer were carried out using the DENZO and SCALEPACK software suites¹⁹ whereas data collected using I19 were processed using Agilent CrysAlis Pro version 171.36.28²⁰. The structures of the new Mn^{2+} polymorph was solved using direct methods in SIR92²¹ and all structures refined using CRYSTALS²².

Powder neutron diffraction measurements were carried out on the high-resolution Wish diffractometer at the ISIS neutron source, Rutherford Appleton Laboratory.²³ The samples were well ground immediately before the measurement and loaded in vanadium cans of either 6 mm or, in the case of $\text{NH}_4\text{Fe}(\text{HCO}_2)_3$, 9 mm diameter. Measurements were carried out between 300 K and 1.5 K with the sample cooled using the standard low-background ^4He cryostat utilised on the beamline; for the $\text{NH}_4\text{Fe}(\text{HCO}_2)_3$ sample data was only collected below 20 K due to the high background from the incoherent scattering from hydrogen. The obtained data were fitted using the Rietveld method as implemented in the GSAS refinement package²⁴ via the EXPGUI interface,²⁵ with appropriate restraints and constraints applied (see ESI for further information). Likely magnetic structures were determined using the ISODISTORT software suite²⁶ by exploring the magnetic distortion modes and symmetries consistent with the observed

k -vector. These, and other possibilities, were then refined as a separate phase, of $P1$ symmetry, in GSAS with constraints applied on the magnetic spin orientation as necessary.

Results and Discussion

Synthesis and Polymorphism

Throughout this work it was found to be difficult to make the $\text{NH}_4\text{B}(\text{HCO}_2)_3$ compounds in pure form with the dominant impurity phase found to be $\text{B}(\text{HCOO})_2 \cdot 2\text{H}_2\text{O}$.²⁷ The quantity of this impurity could be significantly decreased by reducing the quantity of water in the reaction mixture, its formation was, however, unexpected as neither the study of Xu *et al.*¹⁴ or Wang *et al.*¹³ reported its presence despite their use of aqueous ammonia. Neutron diffraction patterns indicated that the $\text{ND}_4\text{Ni}(\text{DCO}_2)_3$ sample used for this study was made in pure form (see Fig. S1) while $\text{NH}_4\text{Fe}(\text{HCO}_2)_3$ contained a significant amount of an unknown impurity (see Fig. S2). Rietveld fits to patterns obtained from samples of $\text{ND}_4\text{Co}(\text{DCO}_2)_3$ and $\text{ND}_4\text{Mn}(\text{DCO}_2)_3$, respectively, indicated they contained 17.80(13) and 21.14(12) weight % of the dihydrate impurity (see Fig. S3 and S4). Additionally the $\text{ND}_4\text{Mn}(\text{DCO}_2)_3$ sample contained 12.21(11) weight % of a new polymorph of $\text{ND}_4\text{Mn}(\text{DCO}_2)_3$, isostructural with $\text{NH}_4\text{Cd}(\text{HCO}_2)_3$,²⁸ which we were unable to isolate in pure form (see Fig. 1 for structure and ESI for further details).

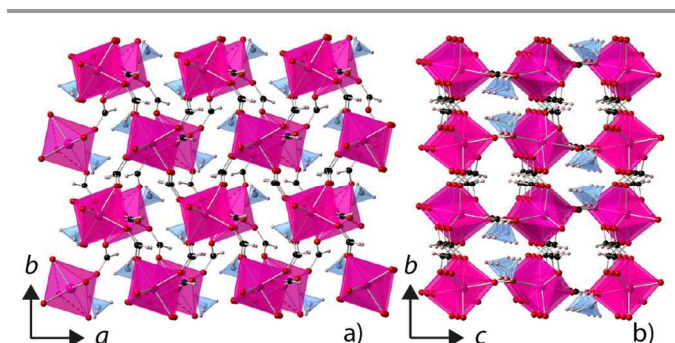


Fig. 1 Structure of the new $\text{NH}_4\text{Mn}(\text{HCO}_2)_3$ polymorph showing the a) ab plane and b) the bc plane. The Mn^{2+} and N atoms, and the polyhedra noting their coordination environment, are dark pink and blue, respectively. The C, O and H atoms are black, red and light pink, respectively.

Crystal Structure of the Ammonium Transition Metal Formates

Fits to neutron diffraction patterns collected from $\text{ND}_4\text{B}(\text{DCO}_2)_3$ ($\text{B} = \text{Co}^{2+}$ and Ni^{2+}) at 250 K and $\text{ND}_4\text{Mn}(\text{DCO}_2)_3$ at 300 K confirmed these phases adopt $P6_322$ symmetry near room temperature. Previously reports of these structures, however, featured ammonium molecules, which resembled heavily distorted trigonal prisms in which only two-thirds of the H-sites are occupied.^{11,13} This is an unusual geometry for an ammonium cation to adopt so, using the much higher sensitivity of neutron diffraction to hydrogen positions, we examined the Fourier difference maps calculated from our refinements if the ammonium positions are excluded from the structure. Additional nuclear density was observed for all three compounds consistent with a hydrogen position on a $4e$ site at

about 1 Å from the nitrogen position (see Fig. 2). This result is most significant for the $\text{ND}_4\text{Ni}(\text{DCO}_2)_3$ sample, which has been synthesised in pure form, and therefore can not be an artefact in the data due to the present of an impurity.

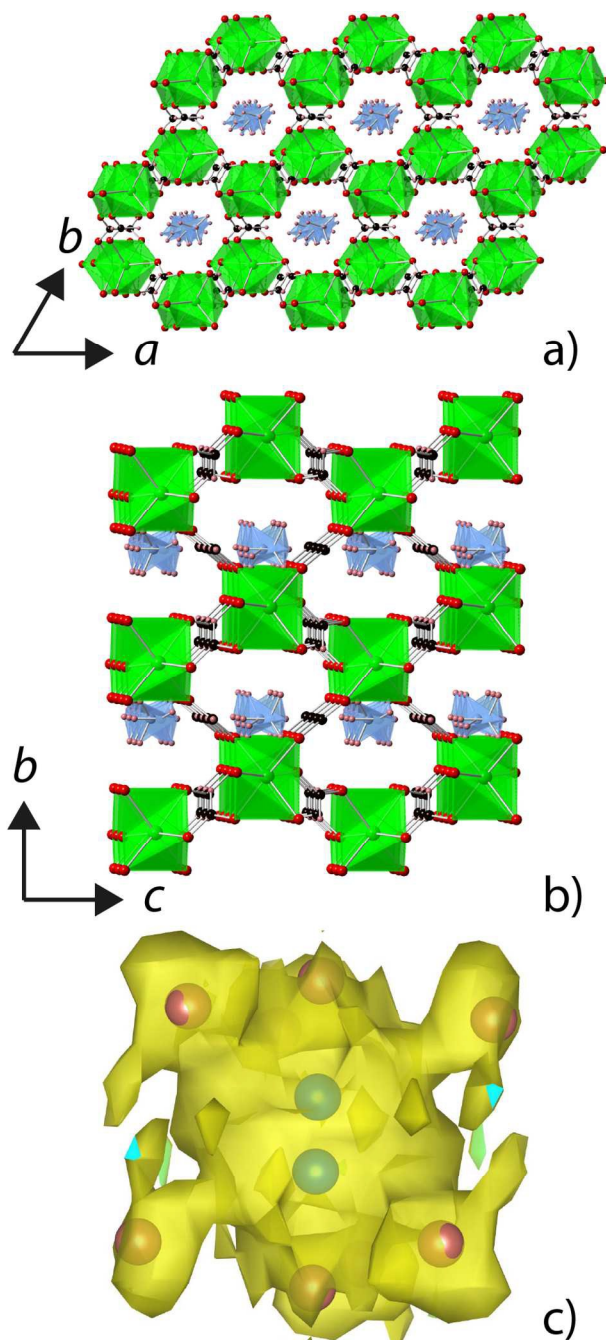


Fig. 2 The structure of $\text{ND}_4\text{Ni}(\text{HCO}_2)_3$ showing a) the hexagonal channels along the c -axis, b) the two disordered ammonium positions and c) the Fourier difference map around the ammonium molecule with a isosurface level of 0.235.

In the previously reported structures for these MOFs the N atom had a very elongated displacement parameter along the c -axis.^{11,13} Consistent with this we observed the nuclear density near the nitrogen sites to be elongated along this direction (see Fig. 2). Given the deuterium positions were well located in the

structure it seems likely that the nitrogen atoms are offset from the ideal $2b$ site onto a neighbouring $4e$ site, which is half occupied, although the resolution of our Fourier maps is not high enough to observe any splitting of the observed nuclear density. The difference in terms of the quality of the fit of our model and the previous model to the data is subtle (e.g. a R_p and R_{wp} of 2.6 and 3.7 % were obtained for both fits to the 250 K dataset of the $\text{ND}_4\text{Ni}(\text{DCO}_2)_3$ framework). We are confident, however, that this is the correct structure as it is more consistent with the Fourier difference maps, it reduces the refined displacement parameters significantly and, critically, is more chemically sound than the previously reported structures. Our models are consistent with the presence of either statically disordered tetrahedral ammonium molecules in the channels or disorder between two equilibrium positions with the ammonium cations spending most of their time in one of these two positions - that is oriented in opposite directions along the c -axis and displaced slightly relative to each other. Resonant ultrasound measurements and broadening of infrared and Raman spectra suggest the NH_4 molecules in the Zn^{2+} and Mg^{2+} analogues are somewhat dynamic so it is likely rapid switching between these two equilibrium positions does occur.²⁹ Ammonium cations in a channel likely orientate in the same direction to avoid unfavourable H-H interactions between apical hydrogen atoms but closest contacts between these in ammonium molecules oriented in opposite directions are greater than 2.5 Å so it is not necessary sterically.³⁰

The only hydrogen bonds short enough to be significant, as previously reported, are between the basal hydrogen atoms of the ammonium cations and the oxygen atoms of the formate ligands.^{11,13} These vary between 1.8 and 1.9 Å depending on composition and temperature, which is shorter than the mean hydrogen bond distance of 1.9 Å reported in the Cambridge Structural Database, as determined by the study of Taylor *et al.*³¹, suggesting these are relatively strong interactions. Assuming the deuterium sites are half occupied, as required by our model, our refinements indicate that the ammonia molecules in $\text{ND}_4\text{Mn}(\text{DCO}_2)_3$, $\text{ND}_4\text{Co}(\text{DCO}_2)_3$ and $\text{ND}_4\text{Ni}(\text{DCO}_2)_3$ were 80.0(5) %, 84.1(4) % and 74.2(7) % deuterated, respectively. The much less labile formate groups were found to be fully deuterated. Overall at most these samples have 6 % of ^1H atoms, leading to only a very small level of incoherent scattering crucial to the high quality neutron diffraction data collected (see Fig S1,S2 and S4) crucial for the analysis contained herein.

The neutron diffraction patterns of the $\text{ND}_4\text{B}(\text{DCO}_2)_3$ ($\text{B} = \text{Mn}^{2+}$, Fe^{2+} and Co^{2+}) samples collected at lower temperatures contain a number of additional reflections indicative of a transition to the polar $P6_3$ phase (see Fig. 3a). These reflections appear at 250 and 200 K for the Mn^{2+} and Co^{2+} phases, broadly consistent with the previously reported transitions in these compounds.¹¹ There is, however, no evidence for a similar transformation in the $\text{ND}_4\text{Ni}(\text{DCO}_2)_3$ framework as the additional reflections indicative of the lower symmetry cell are absent down to 1.5 K and those collected above the previously reported Néel temperature are well fitted by the non-polar

phase (see Fig. 3b). We note that the previous study of Xu *et al.*¹¹ did not collect any structural data representative of the low temperature phase for the $\text{NH}_4\text{Ni}(\text{HCO}_2)_3$ compound and that, unlike the other frameworks in this series the only evidence for a phase transition in the Ni^{2+} compound comes from differential scanning calorimetry (DSC). Moreover the reported transition temperature appears to clearly increase with increasing ionic radii, with the Ni^{2+} framework the only clear exception to this trend.^{11,14,15} It appears from our study that the ionic radii of Ni^{2+} is instead low enough to suppress the polar transition. The Fourier difference maps near the ammonium molecules in the Ni^{2+} framework obtained from fits to data collected at 40 K do not reveal any significant changes, consistent with our model. Indeed the refined displacement of the N from the ideal $2b$ site increases on cooling from 0.0238(11) to 0.0346(6) fractional c -axis coordinates, consistent with freezing in of static disorder.

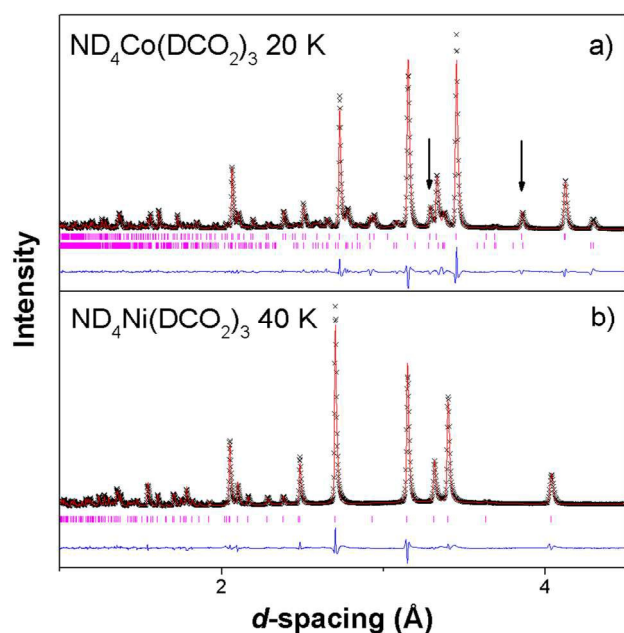


Fig. 3 Diffraction patterns of a) the $P6_3$ polar phase adopted by $\text{ND}_4\text{Co}(\text{DCO}_2)_3$ with the two most intense reflections indicative of this low symmetry phase indicated by arrows and b) of $\text{ND}_4\text{Ni}(\text{DCO}_2)_3$ indicating it maintains the high temperature $P6_322$ phase to low temperature. The black crosses represent the experimental data and the upper red and lower blue lines are the calculated Rietveld fits and the difference profile. The purple vertical markers represent the Bragg reflection markers of the appropriate $\text{ND}_4\text{B}(\text{DCO}_2)_3$ phase. The additional lower set of reflection markers in a) correspond to $\text{Co}(\text{DCO}_2)_3 \cdot 2\text{D}_2\text{O}$.²⁷

The ammonium positions refined in the lower temperature phases against neutron diffraction data from $\text{ND}_4\text{Mn}(\text{DCO}_2)_3$ and $\text{ND}_4\text{Co}(\text{DCO}_2)_3$ are broadly consistent with those in the reported structures.¹¹ Fourier maps show broad but reasonable nuclear density around the ammonium positions in the structure suggestive of well ordered molecules. Synchrotron single crystal X-ray diffraction data obtained from I19 at 30 K, however, revealed some evidence of disorder in the ammonium cations (those containing N3), which fully occupy one third of the channels (see Fig. S5). The retention of some degree of disorder in the ammonium cations in the low temperature $P6_3$

phase would be consistent with the relaxor-like frequency dependence of their observed dielectric permittivities,¹¹ attempts to model two positions in the $\text{NH}_4\text{Co}(\text{HCO}_2)_3$ structure, however, yielded occupancies statistically indistinguishable from 0. The low temperature structures are highly pseudo-symmetric to the parent phase but additional observed reflections confirm the existence of the transitions.

Analysis of the thermal expansion of the $\text{ND}_4\text{B}(\text{DCO}_2)_3$ ($\text{M} = \text{Mn}^{2+}$, Co^{2+} and Ni^{2+}) compounds, using the programme PASCAL,³² show they exhibit anisotropic negative thermal expansion of their c -axis while their a -axis expands on warming (see Fig. 4). Coefficients of thermal expansion of $-22.4(1.7)$, $-18.6(1.1)$ and $-12.7(9)$ MK^{-1} were observed for the Mn^{2+} , Co^{2+} and Ni^{2+} phases between 100 and 250 K (200 K for Co^{2+}), with the magnitude of thermal expansion decreasing significantly at lower temperatures. The thermal expansion values along the a -axis are 21.3(2.2), 19.5(1.6) and 17.0(1.8) MK^{-1} , over the same temperature range. Within this transition metal series it appears that the magnitude of thermal expansion increases with increasing ionic cation radii, although when compared to the Mg^{2+} analogue they are all smaller.¹⁵ Analogous negative linear compressibility of the c -axis has been observed in $\text{NH}_4\text{Zn}(\text{HCO}_2)_3$ and attributed to a wine rack mechanism; this is driven by an increase in the interlayer transition metal angle caused by an increase in rotation of the formate ligands and compression of the M-O bond distance.¹⁶ These structural changes observed under pressure appear to be reversed on heating, suggesting this mechanism may also be responsible for the observed anisotropic negative thermal expansion. The presence of anisotropic negative thermal expansion along the polar c -axis of the Mn^{2+} and Co^{2+} phase, while not unusually large, may improve the ferroelectric properties of these compounds by increasing the ferroelectric displacement of the ammonium cations as the compounds are cooled.

Magnetic Structures of the Ammonium Transition Metal Formates

Additional intensity, that could not be accounted for by the models of the nuclear (crystallographic) phase were observed in diffraction patterns of all four members of the series just below their reported Néel temperature at high d -spacings. This intensity is therefore likely a result of the onset of long-range magnetic order and is only observed in reflections that can be indexed on the parent crystallographic cell. Patterns from the Mn^{2+} and Co^{2+} phase at these low temperatures, however, feature intensity in the (001) reflections, which are systematically absent in their nuclear structure due to the presence of the 6_3 screw axis (see Fig. 5a). This suggests that for these compounds this symmetry element must be violated and some component of the magnetic moments must lie in the ab plane. No intensity was observed in the (001) reflection of the Fe^{2+} and Ni^{2+} compounds (see Fig. 5b), so while all four compounds adopt magnetic structures with a propagation vector, k , of 0 there appear to be at least two types of magnetic structures observed.

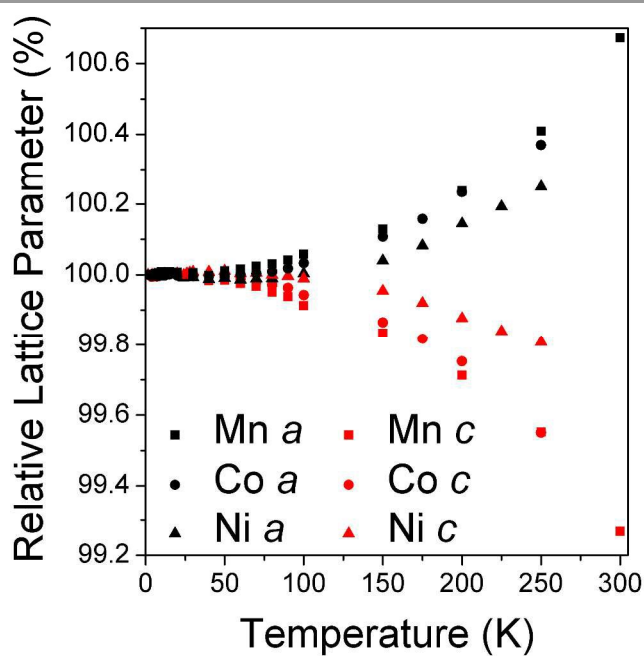


Fig. 4 Relative lattice parameters of the $\text{ND}_4\text{B}(\text{DCO}_2)_3$ frameworks versus temperature. The lattice parameters are scaled to the 1.5 K lattice parameters of the appropriate phase.

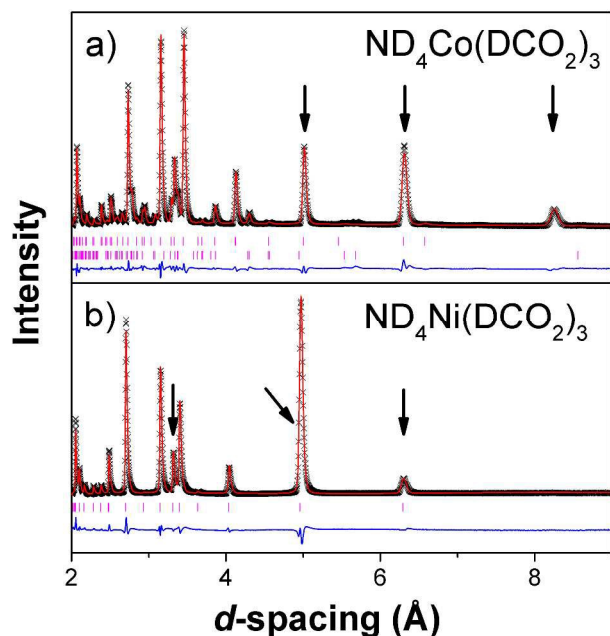


Fig. 5 Neutron diffraction patterns collected at 1.5 K from a) $\text{ND}_4\text{Co}(\text{DCO}_2)_3$ and b) $\text{ND}_4\text{Ni}(\text{DCO}_2)_3$ fitted using the Rietveld method. The format is the same as Fig. 3 and the arrows indicate the three reflections with the most significant magnetic intensity in each pattern, with the (001) reflection present at approximately 8.3 Å in a).

Of the possible models suggested by ISODISTORT²⁶ only one fitted the magnetic intensities observed for the Fe^{2+} and Ni^{2+} compounds with good fits obtained with these magnetic structures (R_p of 0.9 % and 4.3 % and R_{wp} of 0.8 % and 4.8 % for the Fe^{2+} and Ni^{2+} phases were observed to the 1.5 K datasets, respectively). This model is consistent with

antiferromagnetic coupling of cations across approximately 6.5 Å formate pathways and can alternatively be viewed as planes of ferromagnetic cations perpendicular to the c -axis with neighbouring planes aligned antiferromagnetically (see Fig. 6). In our refined models the magnetic moments are parallel to the c -axis since inclusion of magnetic moment in the ab plane does not significantly improve the fit. Therefore the magnetic space groups of these structures were observed to be $P6_3'$ and $P6_3'22'$ for the Fe^{2+} and Ni^{2+} compounds, respectively (this makes no difference to the observed magnetic structure). These structures arise from distortions belong to the magnetic $m\Gamma_2$ and $m\Gamma_3$ irreducible representations, using Miller and Love notation,³³ of the $P6_3$ and $P6_322$, space groups, respectively.

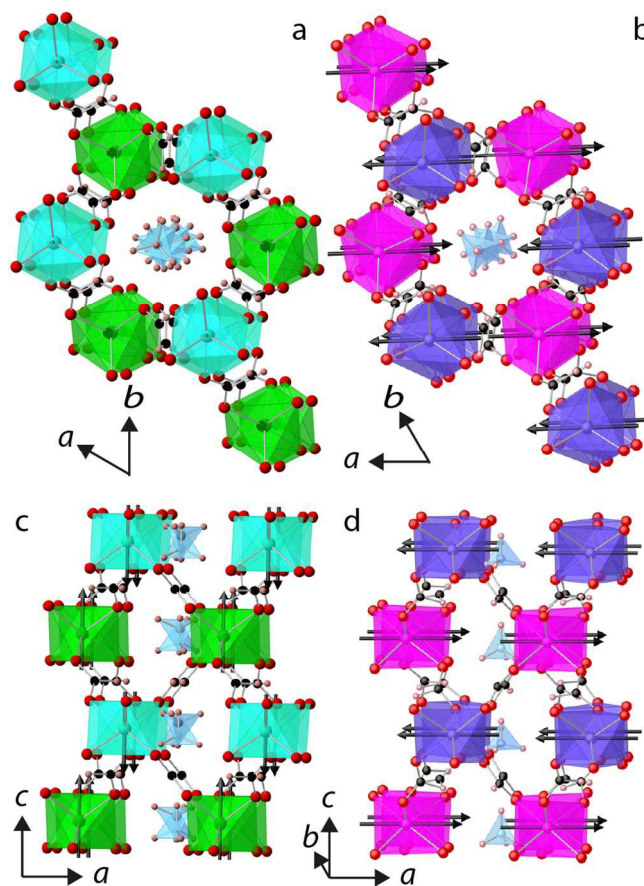


Fig. 6 Magnetic structures of $\text{ND}_4\text{Ni}(\text{DCO}_2)_3$ (a & c) and $\text{ND}_4\text{Co}(\text{DCO}_2)_3$ (b & d) showing the different spin orientations in these two compounds. The spins in $\text{ND}_4\text{Co}(\text{DCO}_2)_3$ are arbitrarily oriented along the a -axis for simplicity and the two differently coloured octahedral in each figure correspond to the two spin orientations in the antiferromagnetic lattice.

The magnetic structures established for the Fe^{2+} and Ni^{2+} compounds are unable to account for the intensity in the (001) reflection so alternate models were tried for the Mn^{2+} and Co^{2+} frameworks. As for the Fe^{2+} and Co^{2+} phases only models with antiferromagnetic cations coupled via formate bridges fitted the data and the magnetic moments must also be co-linear in the ab plane to correctly model the intensity of the (001) reflection. This must necessarily lower the magnetic structure to monoclinic symmetry (see Fig. 6 and S6). Inclusion of a

component of magnetic moment oriented along the c -axis did not considerably improve the quality of the fit. We are, unfortunately, unable to distinguish which direction the moments lie in the ab plane. Our diffraction patterns are essentially hexagonal and the quality of the fits obtained from our refinements are equivalent regardless of whether the moments are aligned along the [100] or [210] directions, the two extreme orientations in the ab plane of a hexagonal structure (for example fits to the 4 K diffraction pattern from the Co^{2+} sample with moments oriented along the [100] or [210] directions gave R_p values of 3.9 % and 3.8 %, respectively, and equivalent R_{wp} values of 4.3 %). The magnetic structure can be identified in ISODISTORT²⁶ as arising from a mixture of two distortion modes belonging to either $m\Gamma_3\Gamma_5$ or $m\Gamma_4\Gamma_6$ depending on whether the moments lie along the [100] or [210] directions, leading to magnetic structures in $P2_1$ and $P2_1'$, respectively. The (100) reflection emerges with the other magnetic reflections at 6 K and 9 K, for Mn^{2+} and Co^{2+} phases respectively, well above the Néel temperature of the major dehydrate impurities.²⁷ Indeed the appearance of the additional reflections well above the Néel temperature of the known impurities in these samples and their failure to index on any reasonable commensurate supercell confirms that the impurities present in these samples are not obfuscating the analysis of the magnetic structures of these materials.

The refined magnetic moment of the Mn^{2+} and Ni^{2+} compounds at 1.5 K, 5.01(4) and 2.23(3) μ_B , are very close to that expected from previous magnetic susceptibility measurements (see Fig. 7 for the magnetic moment temperature dependence).¹³ In contrast the moments obtained for the Fe^{2+} and Co^{2+} cations, 2.36(7) and 2.27(3) μ_B are much lower than would be expected, even if the likely significant orbital contribution to the moments are neglected. Such a result has previously been observed for magnetically frustrated systems³⁴ and previously reported magnetic susceptibility measurements of the Co^{2+} framework suggest it does indeed feature a moderate magnetic frustration index of 5.9, measured as the Curie-Weiss temperature divided by the Néel temperature.¹³ Unfortunately we are insensitive to the spin canting previously indicated to be present in this family of compounds. This is not surprising as the magnitude of the canting, previously attributed as arising from Dzyaloshinsky-Moriya interactions, has been reported to be less than 1° .¹³

The change in orientation of the magnetic moment across the series is completely unexpected. The Mn^{2+} and Co^{2+} compounds, with d^5 and d^7 configurations, have magnetic moments lying in the ab plane while the moments in the Fe^{2+} and Ni^{2+} compounds, which have d^6 and d^8 configurations, are aligned along the c -axis. At first glance a seemingly analogous trend is observed in the monoclinic $\text{B}(\text{HCOO})_2 \cdot 2\text{H}_2\text{O}$ frameworks.^{27,35} Here there are two distinct cations and the Fe^{2+} and Ni^{2+} compounds have antiferromagnetic spins lying in the ac plane slightly canted along the b -axis. These elements of the magnetic structure reverse in the Co^{2+} compound and high temperature Mn^{2+} magnetic phase. The direction of the spins in the ac plane, however, varies across the series and this leads to

the alignment of the Fe^{2+} and Co^{2+} magnetic moments along an octahedral direction, as might be expected from their high single ion anisotropy while the Mn^{2+} and Ni^{2+} structures with lower single ion anisotropy do not. In the title series, however, the differences in the spin direction adopted is not consistent with being driven by single-ion anisotropy. The spins of the Fe^{2+} cation are along a non-octahedral direction, despite its high single ion anisotropy, which is the same orientation as in the Ni^{2+} phase. There are no other clear magneto-structural correlations; for example while the a/c ratio is known to effect the magnetic structure of some metal oxides³⁶ there is no such clear trend here. The a/c ratio of the Fe^{2+} framework is 1.510, which lies between that of Mn^{2+} and Co^{2+} (1.479 and 1.529, respectively) compounds. The cause of this unprecedented alternation of magnetic structures across the series is, therefore, unknown and highlights the need to examine the magnetic structures of other series of formate frameworks in-order to better understand the nature of the magnetic interactions in MOFs since much of this is currently extrapolated from our understanding of simpler magnetic systems with one atom super-exchange bridges, such as oxides.

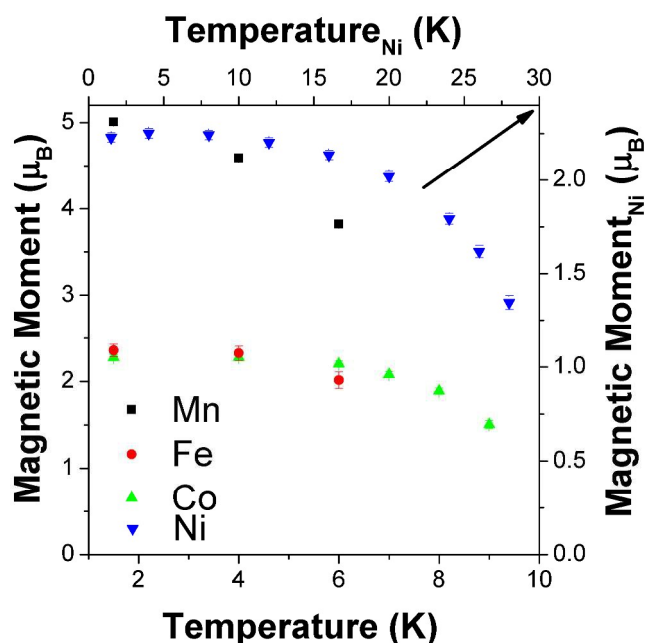


Fig. 7 Evolution of the refined magnetic moment per transition metal cation in the $\text{ND}_4\text{B}(\text{DCO}_2)_3$ frameworks.

Conclusions

We have examined the magnetic interactions in the $\text{NH}_4\text{M}(\text{HCO}_2)_3$ ($\text{M} = \text{Mn}^{2+}, \text{Fe}^{2+}, \text{Co}^{2+}$ and Ni^{2+}) frameworks by determining the magnetic structures of these compounds, a rare systematic study of a family of MOF magnetic structures. We have found that all four frameworks have cations antiferromagnetically coupled to their six nearest-neighbours through formate bridges. The spin orientation, however, changes in an unprecedented way across the series with Fe^{2+} and Ni^{2+} compounds having spins parallel to the c -axis while

those of the Mn^{2+} and Co^{2+} compounds are perpendicular to this, lying in the *ab* plane. We have also unearthed new details regarding the order-disorder transition in this series. In conflict with previous report, we find that the Ni^{2+} framework in this family does not undergo a transition to the polar $P6_3$ phase at lower temperatures, likely due to the smaller size of the B-site cation. The positions of the ammonium cations in the high temperature phase appear to be consistent with the ammonium cations spending the bulk of their time in two positions. We have also quantified the anisotropic negative linear expansion of these transition metal formates, which is exhibit along their polar axis and may therefore enhance their ferroelectric properties.

Acknowledgements

Experiments at the ISIS Pulsed Neutron Source were supported by a beamtime allocation from the Science and Technology Facilities Council. We thank Diamond Light Source for an award of beamline on I19 (MT9981) and thank beamline scientists for their support. PJS would like to thank the Glasstone Bequest for financial support through the provision of a Glasstone Fellowship.

Notes and references

^a Department of Chemistry, University of Oxford, Inorganic Chemistry Laboratory, South Parks Road, Oxford, OX1 3QR, UK. Email: paul.saines@chem.ox.ac.uk

^b ISIS Facility, Rutherford Appleton Laboratory, Harwell, Didcot, OX11 0QX U.K.

Electronic Supplementary Information (ESI) available: Plots of powder diffraction patterns, crystallographic details, including crystallographic information files of the structures determined by single crystal diffraction, and further discussion of synthetic conditions used and details of Rietveld refinements are available. See DOI: 10.1039/b000000x/

- W. Eerenstein, N. D. Mathur and J. F. Scott, *Nature*, 2006, **442**, 759-765.
- J. Glanz, *Science*, 1998, **279**, 2045.
- Y.-Z. Zheng, G.-J. Zhou, Z. Zheng and R. E. P. Winpenny, *Chem. Soc. Rev.*, 2014, **43**, 1462-1475.
- a) G. J. Halder, C. J. Kepert, B. Moubaraki, K. S. Murray and J. D. Cashion, *Science*, 2002, **298**, 1762-1765; b) D. MasPOCH, D. Ruiz-Molina, K. Wurst, N. Domingo, M. Cavallini, F. Biscarini, J. Tejada, C. Rovira and J. Veciana, *Nat. Mater.*, 2003, **2**, 190-195; c) M. G. Warner, C. L. Warner, R. S. Addleman and W. Yantasee, *Magnetic Nanomaterials for Environmental Applications*, 2009.
- a) M. Kurmoo, *Chem. Soc. Rev.*, 2009, **38**, 1353-1379; b) P. J. Saines, M. Steinmann, J.-C. Tan, W. Li, P. T. Barton and A. K. Cheetham, *Inorg. Chem.*, 2012, **51**, 11198-11209; c) P. J. Saines, P. T. Barton, P. Jain and A. K. Cheetham, *CrystEngComm*, 2012, **14**, 2711-2720.
- a) G. Rogez, N. Viart and M. Drillon, *Angew. Chem. Int. Ed.*, 2010, **49**, 1921-1923; b) Z. Wang, K. Hu, S. Gao and H. Kobayashi, *Adv. Mater.*, 2010, **22**, 1526-1533;
- a) Z. Wang, B. Zhang, H. Fujiwara, H. Kobayashi and M. Kurmoo, *Chem. Commun.*, 2004, 416-417; b) M. Kurmoo, H. Kumagai, K. W. Chapman and C. J. Kepert, *Chem. Commun.*, 2005, 3012-3014.
- P. J. Saines, P. T. Barton, M. Jura, K. S. Knight and A. K. Cheetham, *Mater. Horiz.*, 2014, **1**, 332-337.
- G. Lorusso, J. W. Sharples, E. Palacios, O. Roubeau, E. K. Brechin, R. Sessoli, A. Rossin, F. Tuna, E. J. L. McInnes, D. Collison and M. Evangelisti, *Adv. Mater.*, 2013, **25**, 4653-4656.
- P. Jain, V. Ramachandran, R. J. Clark, H. D. Zhou, B. H. Toby, N. S. Dalal, H. W. Kroto and A. K. Cheetham, *J. Am. Chem. Soc.*, 2009, **131**, 13625-13627.
- G.-C. Xu, W. Zhang, X.-M. Ma, Y.-H. Chen, L. Zhang, H.-L. Cai, Z.-M. Wang, R.-G. Xiong and S. Gao, *J. Am. Chem. Soc.*, 2011, **133**, 14948-14951.
- L. Cañadillas-Delgado, O. Fabelo, J. A. Rodríguez-Velamazán, M.-H. Lemée-Cailleau, S. A. Mason, E. Pardo, F. Lloret, J.-P. Zhao, X.-H. Bu, V. Simonet, C. V. Colin and J. Rodríguez-Carvajal, *J. Am. Chem. Soc.*, 2012, **134**, 19772-19781.
- Z. Wang, B. Zhang, K. Inoue, H. Fujiwara, T. Otsuka, H. Kobayashi and M. Kurmoo, *Inorg. Chem.*, 2006, **46**, 437-445.
- G.-C. Xu, X.-M. Ma, L. Zhang, Z.-M. Wang and S. Gao, *J. Am. Chem. Soc.*, 2010, **132**, 9588-9590.
- R. Shang, G.-C. Xu, Z.-M. Wang and S. Gao, *Chem. Eur. J.*, 2014, **20**, 1146-1158.
- W. Li, M. R. Probert, M. Kosa, T. D. Bennett, A. Thirumurugan, R. P. Burwood, M. Parinello, J. A. K. Howard and A. K. Cheetham, *J. Am. Chem. Soc.*, 2012, **134**, 11940-11943.
- a) P. J. Saines, J. R. Hester and A. K. Cheetham, *Phys. Rev. B*, 2010, **82**, 144435; b) P. J. Saines, B. C. Melot, R. Seshadri and A. K. Cheetham, *Chem. Eur. J.*, 2010, **16**, 7579-7585; c) O. Fabelo, L. Cañadillas-Delgado, I. s. Puente Orench, J. A. Rodríguez-Velamazán, J. Campo and J. Rodríguez-Carvajal, *Inorg. Chem.*, 2011, **50**, 7129-7135; d) O. Fabelo, L. Cañadillas-Delgado, J. Pasán, P. Díaz-Gallifa, C. Ruiz-Pérez, F. Lloret, M. Julve, I. Puente Orench, J. Campo and J. Rodríguez-Carvajal, *Inorg. Chem.*, 2013, **52**, 12818-12827; e) R. A. Mole, M. A. Nadeem, J. A. Stride, V. K. Peterson and P. T. Wood, *Inorg. Chem.*, 2013, **52**, 13462-13468.
- H. Nowell, S. A. Barnett, K. E. Christensen, S. J. Teat and D. R. Allan, *J. Synchrotron Radiat.*, 2012, **19**, 435-441.
- Z. Otwinowski and W. Minor, in *Methods in Enzymology*, ed. Charles W. Carter, Jr., Academic Press, 1997, vol. Volume 276, pp. 307-326.
- CrysAlis PRO* 171.36.28, Agilent Technologies, Yarnton, Oxfordshire, England, 2013.
- A. Altomare, G. Casciarano, C. Giacovazzo, A. Guagliardi, M. C. Burla, G. Polidori and M. Camalli, *J. Appl. Crystallogr.*, 1994, **27**, 435.
- P. W. Betteridge, J. R. Carruthers, R. I. Cooper, K. Prout and D. J. Watkin, *J. Appl. Crystallogr.*, 2003, **36**, 1487.
- L. C. Chapon, P. Manuel, P. G. Radaelli, C. Benson, L. Perrott, S. Ansell, N. J. Rhodes, D. Raspino, D. Duxbury, E. Spill and J. Norris, *Neutron News*, 2011, **22**, 22-25.
- A. C. Larson and R. B. Von Dreele, *General Structure Analysis System (GSAS)*, Los Alamos National Laboratory Report LAUR 86-748, Los Alamos National Laboratory, Los Alamos, 1994.
- B. Toby, *J. Appl. Crystallogr.*, 2001, **34**, 210-213.
- B. J. Campbell, H. T. Stokes, D. E. Tanner and D. M. Hatch, *J. Appl. Crystallogr.*, 2006, **39**, 607-614.

27. P. Burel, P. Burel, J. Rossat-Mignot, A. De combarieu and E. Bedin, *Phys. Status Solidi B*, 1975, **71**, 675-685.
28. A. S. Antsyshkina, M. A. Porai-Koshits, V. N. Ostrikova and G. G. Sadikov, *Koordinats. Khim.*, 1983, **9**, 855-858.
29. a) M. Mączka, A. Pietraszko, B. Macalik and K. Hermanowicz, *Inorg. Chem.*, 2014, **53**, 787-794; b) Z. Zhang, W. Li, M. A. Carpenter, C. J. Howard and A. K. Cheetham, *CrystEngComm*, 2015.
30. P. A. Wood, J. J. McKinnon, S. Parsons, E. Pidcock and M. A. Spackman, *CrystEngComm*, 2008, **10**, 368-376.
31. R. Taylor, O. Kennard and W. Versichel, *Acta Crystallogr. B*, 1984, **40**, 280-288.
32. M. J. Cliffe and A. L. Goodwin, *J. Appl. Crystallogr.*, 2012, **45**, 1321-1329.
33. S. C. Miller and W. F. Love, *Tables of irreducible representations of space groups and co-representations of magnetic space groups*, Pruett Press, Boulder, Colorado, 1967.
34. a) V. Hardy, C. Martin, G. Martinet and G. André, *Phys. Rev. B*, 2006, **74**, 064413; b) C. Yin, G. Li, W. A. Kockelmann, F. Liao, J. P. Attfield and J. Lin, *Chem. Mater.*, 2010, **22**, 3269-3276.
35. M. R. V. Jørgensen, M. Christensen, M. S. Schmøkel and B. B. Iversen, *Inorg. Chem.*, 2011, **50**, 1441-1446.
36. D. A. O. Hope and A. K. Cheetham, *J. Solid State Chem.*, 1988, **72**, 42-51.